



A Synaptic Basis for Paracrine Interleukin-2 Signaling during Homotypic T Cell Interaction

Catherine A. Sabatos,^{1,3} Junsang Doh,^{1,2,3} Sumone Chakravarti,¹ Rachel S. Friedman,¹ Priya G. Pandurangi,¹ Aaron J. Tooley,¹ and Matthew F. Krummel^{1,*}

¹Department of Pathology, University of California, San Francisco, San Francisco, CA 94143-0511, USA

²School of Interdisciplinary Bioscience and Bioengineering and Department of Mechanical Engineering, Pohang University of Science and Technology, Hyoja-Dong, Nam-Gu, Pohang, Gyeongbuk 790-784, South Korea

³These authors contributed equally to this work

*Correspondence: matthew.krummel@ucsf.edu

DOI 10.1016/j.immuni.2008.05.017

SUMMARY

T cells slow their motility, increase adherence, and arrest after encounters with antigen-presenting cells (APCs) bearing peptide-MHC complexes. Here, we analyzed the cell-cell communication among activating T cells. In vivo and in vitro, activating T cells associated in large clusters that collectively persisted for >30 min, but they also engaged in more transient interactions, apparently distal to APCs. Homotypic aggregation was driven by LFA-1 integrin interactions. Ultrastructural analysis revealed that cell-cell contacts between activating T cells were organized as multifocal synapses, and T cells oriented both the microtubule-organizing complex and interleukin-2 (IL-2) secretion toward this synapse. T cells engaged in homotypic interactions more effectively captured IL-2 relative to free cells. T cells receiving paracrine synaptic IL-2 polarized their IL-2 signaling subunits into the synaptic region and more efficiently phosphorylated the transcription factor STAT5, likely through a synapse-associated signaling complex. Thus, synapse-mediated cytokine delivery accelerates responses in activating T cells.

INTRODUCTION

The stages of T cell trafficking, activation, and arrest have been described in vivo for both CD8+ (Bousso and Robey, 2003; Mempel et al., 2004) and CD4+ (Miller et al., 2002, 2003, 2004) T cells. T cells initially scan dendritic cells (DCs), "searching" for cognate peptide (Lindquist et al., 2004; Shakhar et al., 2005), and subsequently swarm and arrest on DCs (Hugues et al., 2004). The end of this phase coincides with upregulation of CD25 and the initiation of IL-2 secretion from T cells (Mempel et al., 2004). Chemokine secretion, such as CCL3 and CCL4 produced by activated DCs and T cells, increases the likelihood that T cells will commingle in regions where other T cells are currently, or have previously been, localized (Castellino et al., 2006; Hugues et al., 2007). This results in both long-lived and dynamic "clusters" of T cells, responding to immunization (Bousso and Robey, 2003) or autoantigens (Tang et al., 2006). In a third phase, T cells are released

from DCs, migrate once again, and subsequently proliferate and gain effector function.

In vitro, the initiating cell-cell contact between a T cell and an antigen-presenting cell (APC) has been characterized as an immunological synapse (IS) (Grakoui et al., 1999; Monks et al., 1998). Within this contact, clusters of adhesive LFA-1 molecules surround central clusters of T cell receptors (TCRs) (Grakoui et al., 1999; Monks et al., 1998). This stable contact facilitates prolonged signaling as well as polarization of surface proteins (Huppa et al., 2003; Krummel et al., 2000), the cytoskeleton (Bunnell et al., 2002; Kupfer et al., 1983), and secretory machinery (Huse et al., 2006; Stinchcombe et al., 2006) toward the APC.

Despite extensive characterization of the dynamics and nature of T cell activation, the complete impact of arrest and the ensuing changes in both T cell motility and adherence are not well elucidated. As T cells' clustering upon activation has been a hallmark of activated cells both in vivo (Hommel and Kyewski, 2003; Ingulli et al., 1997) and in vitro (Inaba et al., 1984), we reasoned that motility arrest and localized aggregation of T cells might also encourage direct cell-to-cell crosstalk among adjacent activating T cells. We thus sought to characterize the nature of T-T cell surface interactions and the underlying cell biology within T-T clusters.

Here, we present evidence that T-T clusters promote synapse-based cytokine delivery between activating T cells. LFA-1-mediated multifocal synapses promote the polarization of microtubule-organizing centers and direct cytokine secretion toward adjacent T cells. These interactions are functionally important as they facilitate synapse-localized signaling complexes and activation of STAT5, a transcription factor downstream of IL-2R signaling.

RESULTS

Prolonged Cell-Cell Contacts between Activated T Cells In Vivo

To gain greater insight into the dynamic nature of T cell clustering, we immunized mice with peptide in adjuvant and imaged excised lymph nodes (LNs) to specifically analyze T-T dynamics during swarming and arrest. We adoptively transferred CFSE-labeled DO11.10 CD4⁺ T cells into wild-type (WT) BALB/c recipients and activated the cells by subcutaneous (s.c.) immunization 24 hr later with OVA 323-339 (OVA 323) emulsified in complete Freund's adjuvant (CFA). As a control for immunization effects, we also analyzed LN draining of an equivalent volume of



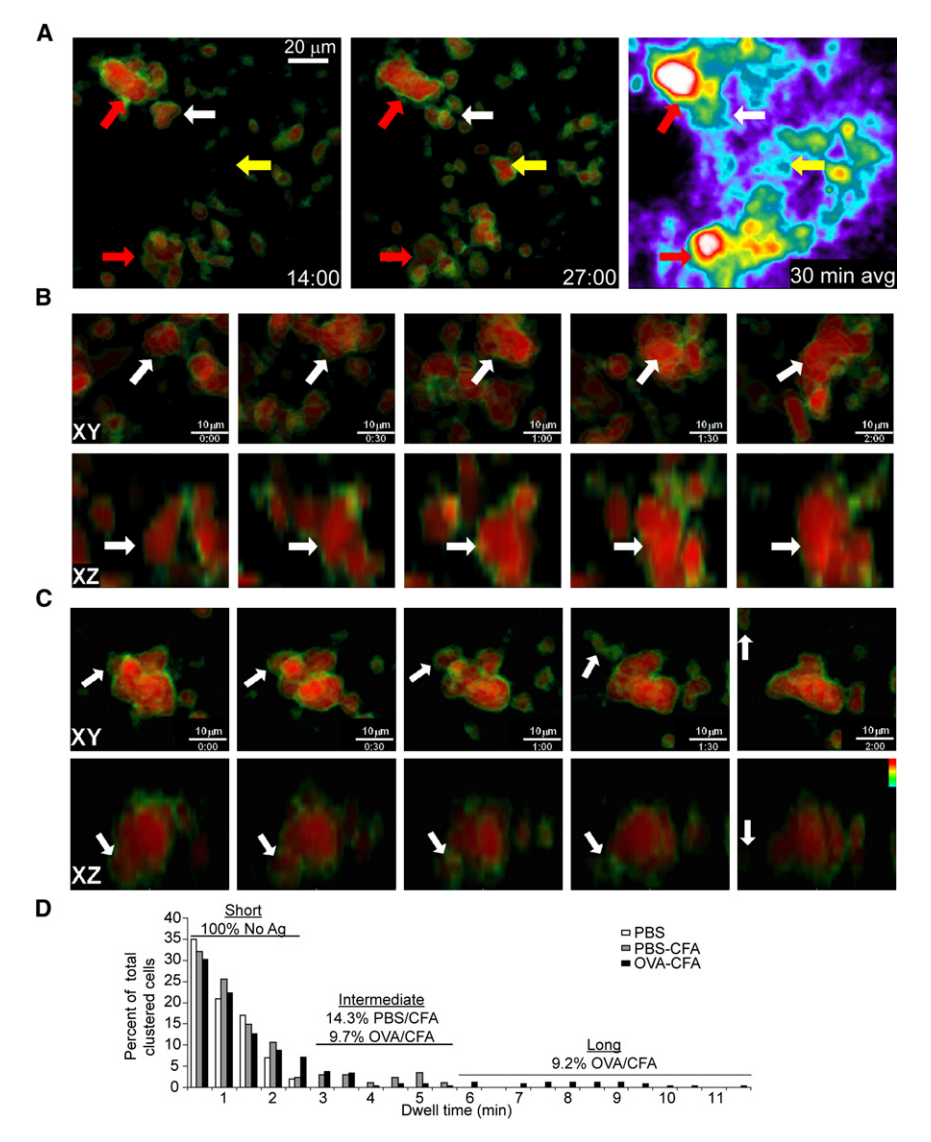


Figure 1. Swarming Activation Clusters during TCR-Dependent T Cell Activation In Vivo

Explant popliteal lymph nodes (LNs) from wildtype (WT) BALB/c mice injected with CFSE-labeled DO11.10 T cells were removed 24 hr after OVA-CFA immunization and imaged for 30 min time lapses. Data are representative of six or more independent experiments. Time stamp = min:s.

(A) Projection images of 312 μ m (x) × 260 μ m (y) × 150 μ m (z)-deep data stack. Left two panels: large "stable" (red arrows) and small "transient" (white and yellow arrows) clusters are shown at two time points in which CFSE is pseudocolored (black/green/yellow/red) on a scale that highlights the cell borders as a result of their slightly reduced fluorescence intensity. Right panel: time average of an entire 30 min run showing the spatial persistence of cells in the two "stable" clusters and only weak persistence of cells in the smaller clusters. (B and C) Cropped data of two large clusters showing fusion and dispersal.

(B) Fusion of a midsize cluster (estimated to contain 3–4 cells initially) with other individual and clustered T cells over a 2 min period. Viewing xy and xz projections of the cluster (indicated by arrow) permits the same cluster to be observed as other clusters and cells join from multiple directions

(C) A single T cell leaves a cluster and crawls away over a 2 min period. Note the appearance of the green border around the departing cell at min 1, indicative of the movement out of the cluster in xy (upper panels) and xz (lower panels) dimensions.

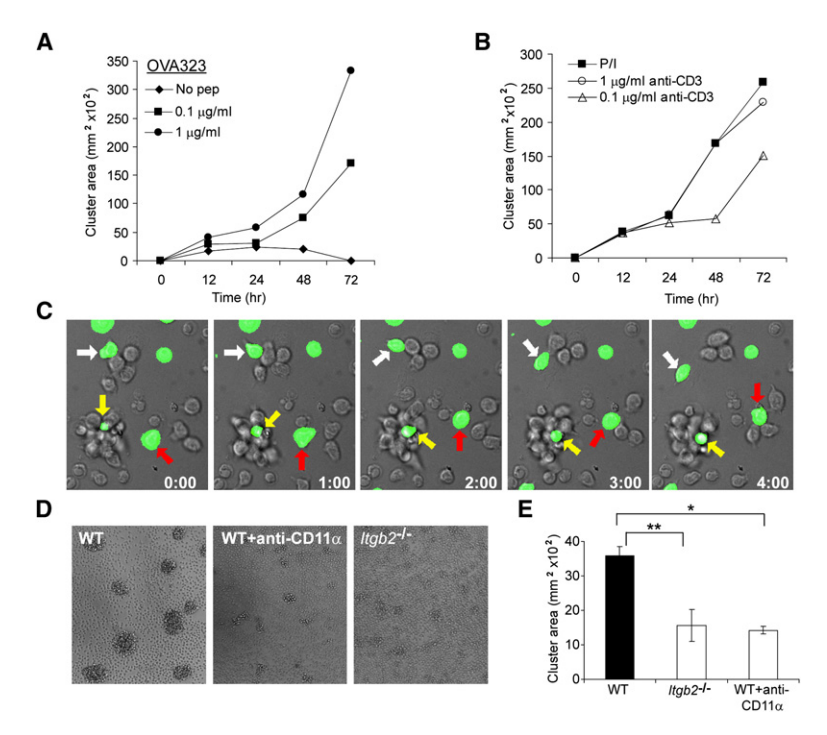
(D) Dwell time of transient "small" clusters as a function of immunization condition. Any close T-T contact was scored for the length of interaction prior to dispersal and represented as a percent of total T-T interactions scored. PBS only, unimmunized control; OVA-CFA, draining LN; PBS-CFA, control immunized LN. At least 19 couples were scored for each condition.

phosphate-buffered saline (PBS) and CFA. After 24 hr, popliteal draining (OVA-CFA) and nondraining (PBS-CFA) LNs were excised, mounted to coverslips, and imaged by two-photon laser scanning microscopy (TPLSM). In Figure 1, we show CFSE on a pseudocolor scale where the center of the T cell body appears red and the fainter outer region of the cell (typically dimmer because the CFSE is fainter at or just beyond the pixels bearing membrane) is color coded green. This display highlights close associations; the green border is lost at points where the cell bodies become closely apposed (see Figures 1A-1C). We found large (>3 cells, often much larger) clusters of T cells deep within the LN (>150 µm below the capsule), with persistent interactions in the draining LN (Figure 1A, red arrows) that remained occupied by T cells for a full 30 min (see Movie S1 available online). The frequency of the very large clusters was variable, but over >5 experiments scored, we found an average of 6.6 per mm³ of the large clusters shown in Figure 1A per LN surveyed, 18-22 hr after immunization. Though persistent on the whole, these large clusters were also somewhat dynamic, with ongoing evidence of coalescence, for example when multiple clusters joined (Figure 1B) or individual cells dissociated (Figure 1C; Movie S2) from existing clusters. Notably, unactivated (antigen-nonspecific) cells did not participate in these clusters to the same degree as activated cells (Movie S3).

The ability of T cells to self-associate for longer times was not purely confined to these large clusters. We also observed transient contacts that occurred when individual or small numbers of motile T cells in this phase encountered one another in regions that were otherwise devoid of labeled cells (Figure 1A, white and yellow arrows). A time average of the entire field demonstrated the local persistence of cells over time at the large clusters, whereas another population of smaller clusters were frequently more transient (Figure 1A, right panel).

For these smaller, more transient aggregates, we measured the length of time that a given T cell remained in close association with another T cell, starting from the point at which we could first see them in close proximity. All of the T-T interactions measured in control mice that received labeled cells transferred without immunization (LNs taken 24 hr posttransfer) were 2.5 min or less in duration (mean 1.0 min), revealing a background of only





is shown as a function of time. Data are representative of two independent experiments. (B) DO11.10 CD4 $^+$ T cells were activated with PMA and ionomycin or titrated plate-bound anti-CD3 with soluble anti-CD28 (5 μ g/ml); cluster formation over time is represented as in (A). Data are representative of two independent experiments.

Figure 2. Dynamic Activation Clusters In Vitro Utilize

(A) Whole DO11.10 LN cells were activated in vitro with titrated

doses of OVA 323 (0-1 µg/ml); wells were photographed at the

indicated time points. The cross-sectional (xy) area of clusters

LFA-1 to Assemble

(C) C57BL/6 CD4⁺T cells (90% unlabeled, 10% CFSE labeled) were stimulated with PMA and ionomycin, and time-lapse microscopy was performed 18 hr after stimulation. Differential interference contrast (DIC) and green fluorescence from CFSE were acquired every 20 s over 5 min. White arrows indicate a dissociating cell, red arrows indicate a cell joining a cluster, and yellow arrows indicate a persistent cluster. Time stamp = min:s.

(D and E) B6 WT or LFA-1-deficient $Itgb2^{-/-}$ CD4* T cells were stimulated for 20 hr with PMA and ionomycin. At 18 hr, some B6 WT cells were treated with anti-CD11 α (LFA-1) antibody (20 μ g/ml). Cluster formation was assessed at 20 hr as above. (D) shows representative pictures of clusters; (E) shows graphical representation of clustering. *, two-sample t(94) = 1.986, p = 1.14 \times 10⁻¹³; **, two-sample t(93) = 1.986, p = 1.75 \times 10⁻¹². Data are representative of two to three independent experiments. Error bars in (E) represent SD.

short T-T interactions (Figure 1D). Immunization in adjuvant led to a population of intermediate-length (3–6.5 min) interactions for both PBS-CFA (14.3%) and OVA-CFA (9.7%), suggesting that inflammation and the ensuing shift toward lower motility (Hugues et al., 2004; Shakhar et al., 2005) favor somewhat longer interactions. Relative to this nonspecific background, peptide-specific immunization (OVA-CFA) gave rise to a population (9.2% of all T-T encounters) with longer kinetics (Figure 1D). Although this population was not large and the maximal duration of these transient T-T clusters rarely exceeded 10 min, if extended over many hours, these small T-T clusters are likely to result in multiple associations for cells during the course of activation.

APC-Dependent or -Independent Stimuli Result in Dynamic LFA-1-Mediated T Cell Cluster Assembly In Vitro

While TPLSM is ideally suited to studying the dynamics of cell-cell association, an in vitro system was required to ascertain the exact nature of the cell-cell contact. By engaging TCRs on T cells in vitro in the presence or absence of APCs, we studied the requirement for APCs in mediating T cell homotypic adhesion.

Whole-LN preparations from DO11.10 mice were activated with titrated doses of OVA peptide, and cluster size was tracked over 72 hr. As with the in vivo setting, activation-induced T-T aggregation began approximately 16 hr after stimulation, and cells joined over time to form larger arrays of T cells in clusters. Clustering kinetics and extent were antigen dose dependent (Figure 2A). Furthermore, self-aggregation by T cells stimulated with either anti-CD3 antibody plus anti-CD28 antibody or phorbol 12-myristate 13-acetate (PMA) plus ionomycin in the absence of APCs indicated that this ability to self-aggregate is a capacity

gained after cell activation but not absolutely requiring a nucleating APC (Figure 2B).

Clusters generated in the absence of APC-based ISs also resembled the in vivo scenario insofar as the T cells in the clusters remained motile and associations were highly dynamic. As shown in Figure 2C and Movie S4, we seeded 10% CFSE-labeled CD4+ C57BL/6 T cells into a culture with identical unlabeled cells and activated them for 18 hr with PMA and ionomycin. The resulting clusters demonstrated both stability (yellow arrow) and plasticity, with T cells both joining (red arrow) and leaving (white arrow) clusters similarly to that seen in vivo. The ongoing cell motility in vitro and high plasticity argue against a random aggregation model and instead suggest that T cells actively engage in stable interactions with one another in the course of ongoing motility and might do so via specific mechanisms, such as integrin-mediated adhesion.

Given that the primary T cell integrin, LFA-1, is required for initiation of activation when APCs are stimulators, we used APC-independent activating stimuli to probe the role of LFA-1 in driving self-aggregation of CD4⁺ T cells. This permitted study of T cells derived from LFA-1-deficient ($Itgb2^{-/-}$) mice or of WT cells in the presence of blocking antibody against LFA-1 (anti-CD11α). There was a significant reduction (two-sample t(93) = 1.986, p = 1.75×10^{-12}) of activation-induced T cell clustering in cells from Itgb2^{-/-}mice (Figures 2D and 2E) activated with PMA and ionomycin as compared to cells from WT mice. After cluster assembly, and in accord with previous studies (Rothlein and Springer, 1986), the addition of CD11α antibody, but not antibodies against other adhesion receptors (including Jam-1, MAC-1, VCAM, α4, and α4β7; data not shown), effectively dispersed these aggregates in WT CD4+ T cells (two-sample t(94) = 1.986, p = 1.14 × 10⁻¹³), demonstrating that LFA-1 serves as a primary source of adhesion for T-T contacts (Figures 2D and 2E). Similar results were observed using anti-CD3 plus



anti-CD28 stimulation (data not shown). This confirmed that T-T clustering in vitro is activation mediated but does not require a bridging DC. Staining of clusters with antibodies to LFA-1 (Figure S1) also showed specific enrichment of this protein in the regions of close juxtaposition, further highlighting that this process is active rather than passive. Notably, only modest enrichment of CD86 (Figure S1), MHC, TCR, CD4, and CD28 (data not shown) was observed in T-T synapses, which contrasts these with the ISs formed between T cells and APCs (Krummel et al., 2000; Monks et al., 1998; Pentcheva-Hoang et al., 2004).

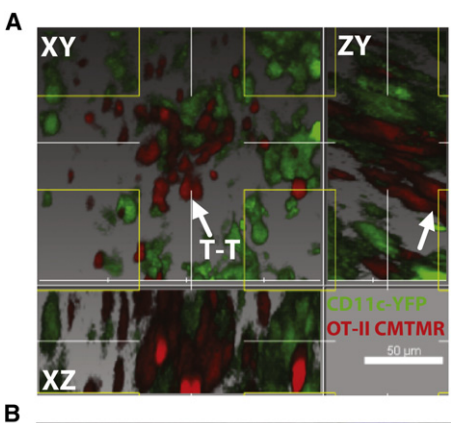
T-T Interactions Proximal and Distal to T-APC Synapses

T-T interactions are activation induced, as evidenced by the requirement both in vitro and in vivo for TCR stimulation preceding T-T clustering (Figure 1; Figure 2). The data in Figure 2 suggested that DCs are not required to mediate homotypic aggregation. However, to determine the relative DC dependence or independence of T-T interactions when stimulation is driven by DCs in vivo or in vitro, we localized DCs within the context of clusters. To achieve this in vivo, we transferred CMTMR-labeled OT-II CD4⁺ T cells into CD11c-YFP mice (Lindquist et al., 2004), immunized s.c. with OVA-CFA, and imaged LN draining via TPLSM after 24 hr. As shown in Figure 3A and Movie S5, the vast majority of T cells form large clusters around DCs, with T cells concurrently engaging in homotypic interactions. We also were able to visualize the smaller cohort of T cells engaging in homotypic interactions at some distance from the nearest DC (Figure 3A). It is worth noting that very thin dendrites may project from the DC in Figure 3A, and so it is not formally possible in this context to exclude a role for DCs in the aggregate. Additionally, given the density of DCs within the T cell zone of the LN, DCs are certainly always very nearby.

Similarly, T-T interactions proximal to and distal from the DC body were observed in vitro when OT-II CD4+ T cells were activated by CFSE-labeled bone marrow dendritic cells (BMDCs) prepulsed with OVA 323. As shown in Figure 3B, T cells packed tightly around central DCs (blue), and additional T cells extended to peripheral parts of the cluster, away from close contact with the nucleating DC. Again, although small dendrites may assist in these contacts, taken together with the data from Figure 2, it appears likely that activating T cells acquire some affinity for one another, independent of DCs.

T-T Contacts Are Mediated by Multifocal Synapses

The T-T cluster requirement for adhesion molecules and formation in the absence of added or apparent APCs both in vivo and in vitro suggested that a homotypic LFA-1-mediated synapse-like structure might facilitate T-T interactions in a fashion similar to T cell-APC synapses. Electron microscopy (EM) analysis demonstrated that T-T synapses formed between activated T cells with strong membrane apposition similar to that seen at a typical IS between a T cell and DC (Brossard et al., 2005) (Figure 4A). Of particular note are the synaptic spaces (arrowheads in Figure 4B) at the contacts, indicative of a multifocal synapse with substantial intercellular volume enclosed by the apposed membranes. Furthermore, EM sections in which intracellular vesicles could be observed frequently showed those vesicles to be oriented toward the adjacent T cells (Figure 4C), further suggesting that these encounters were not passive.



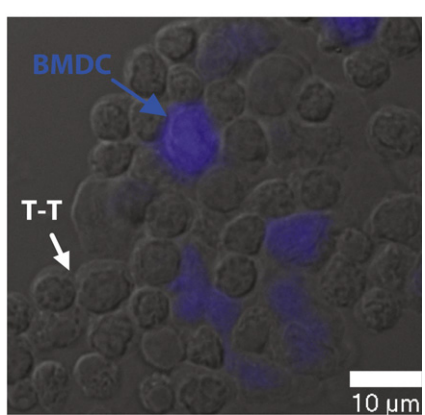


Figure 3. Relationship of T-APC Contacts to T-T Contacts

(A) CMTMR-labeled OT-II CD4+ T cells were injected into CD11c-YFP mice, which were immunized subcutaneously with OVA-CFA, and the draining LN was isolated for TPLSM after 24 hr, corresponding to phase II of T cell activation. A region containing clusters demonstrates a majority of T cells forming simultaneous contacts with antigen-presenting cells (APCs) and one another and a smaller cohort engaging in homotypic interactions at some distance from the nearest dendritic cell (DC). The white arrow indicates a T-T contact distal to adjacent DC cell bodies. Note that the T cell zone contains a meshwork of DCs, and it is highly probable that any T cells will lie within a distance of less than 20 μm from a visible DC body while within this zone, regardless of their potential interactions.

(B) OT-II CD4 $^{\scriptscriptstyle +}$ T cells were activated in vitro for 20 hr with C57BL/6 bone marrow dendritic cells (BMDCs) prelabeled with OVA 323 and CMAC (blue). Note that some lateral T-T interactions occur for T cells directly contacting APCs, whereas additional T cells homotypically interact beyond the evident DC border. Data are representative of at least three independent trials.

Polarized MTOC and Secretion of IL-2 at T-T Synapses

Reorientation of a migrating cell upon pMHC-induced arrest results in the polarization of the Golgi apparatus and microtubule-organizing complex (MTOC) toward the point of contact, allowing for the alignment of intracellular organelles and secretion of effectors into the synapse (Kupfer et al., 1983). Staining for the MTOC-associated protein pericentrin at T-T synapses (Figure 5A) indicated an 80% bias in the polarization of the tubulin cytoskeleton inward toward adjacent T cells. In the right panel of Figure 5A, we assessed whether this bias was due to specific polarization of pericentrin as opposed to simple availability of T-T contact interface versus free membrane. If the bias toward polarization "in" were due simply to a high percentage of available T-T contact interface (versus free membrane), one would predict that



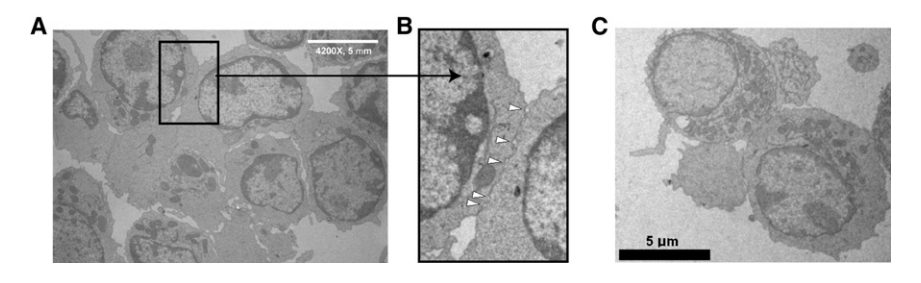


Figure 4. Ultrastructural Features of T-T Clusters

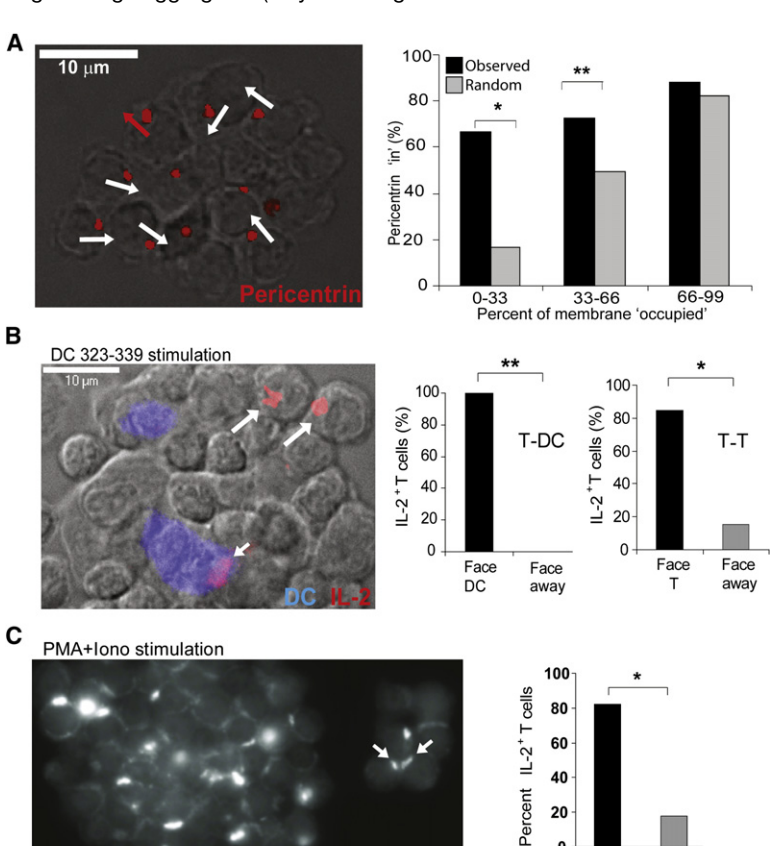
BALB/c WT CD4+ T cells were stimulated with PMA and ionomycin; 18 hr after stimulation, electron microscopy was performed.

- (A) Representative image of interacting T cells. with inset showing a T-T interface.
- (B) Magnification of a T-T synaptic region showing synaptic gaps (arrowheads) between tightly apposed membranes.
- (C) Representative view of cell conjugate showing intracellular vesicles positioned opposite one another in the two primary cells.

the percent of T-T contact would correlate directly to the percentage of protein facing inward (i.e., 10% T-T contact and 90% free membrane results in 10% pericentrin "in" and 90% pericentrin "out"). However, when tested against this hypothesis, the observed percentage of pericentrin facing "in" was significantly higher than that predicted for 0%-33% (p = 0.00001) and 33%–66% (p = 0.002) T-T contact (Figure 5A, graph). This suggested that activating T cells selectively polarize toward one another, potentially to facilitate the organization of effector molecules, secretion, and signaling at T-T interfaces. To directly test whether T-T synapses polarized cytokine secretion, we stained aggregates for intracellular IL-2. As demonstrated previously (Huse et al., 2006), IL-2-containing vesicles were directionally polarized toward APCs when an APC was the neighboring cell (Figure 5B, small arrow). However, when T cells on the edge of large aggregates (only including those where molecules had the "choice" of inward or outward polarization) were examined for the polarization of intracellular IL-2, there was a strong bias (84.6%) in these vesicles toward polarization to an adjacent T cell (Figure 5B, large arrows). Similarly, when large aggregates of T cells, activated independently of APCs by PMA plus ionomycin, were examined, over 80% of all contacts demonstrated strong polarization of IL-2 pools facing inwards (Figure 5C).

T-T Synapses Facilitate Capture of Secreted Cytokines

The data from Figure 5 strongly suggested that T cells in clusters would have a benefit in terms of their exposure to IL-2 as a result of the localized secretion. To test whether this was the case, we took advantage of a "catch" antibody detection system that uses a surface-binding antibody to locally capture IL-2 on the cell that is exposed to it. By coating cells with this antibody prior to activating them with an APC-independent stimulus (Figure 6A,



Face

Face

away

Figure 5. Polarized Secretion and Receptor Aggregates between T Cells in Clusters

(A) Pericentrin is detected facing inward after activation with PMA and ionomycin. DO11.10 CD4⁺ T cells were stimulated for 19 hr with PMA and ionomycin; permeabilized clusters fixed to slides were stained with purified anti-pericentrin antibody. Pericentrin is shown as red dots; white arrows indicate pericentrin stain localized into cluster; red arrows indicate pericentrin pointed outward from T cluster. The graph represents the actual percent of pericentrin "in" (black bars) versus the predicted percent of pericentrin that would be expected to face "in" (gray bars) if the polarization were due to the percent of available T-T membrane interface (x axis). *p = 0.00001, **p = 0.002 by chi-square goodness-of-fit test.

(B) IL-2 is polarized inward toward DC and T contacts in clusters when activated by peptide-pulsed DCs. OT-II CD4+T cells were activated for 20 hr with actin-CFP+ BMDCs prepulsed with OVA 323 (10 μg/ml). Permeabilized clusters were stained with anti-IL-2 antibody. DCs are shown in blue on wide-field DIC overlay and IL-2 in red. In the graphs, IL-2 localization is represented as the percent of IL-2+ T cells pointing toward a DC or away from the DC for all IL-2+ T-DC pairs (left graph) and as the percent of IL-2+ T cells pointing in toward a facing T cell or pointing away from a neighboring T cell for all IL-2+ T-T pairs (only border cells scored) (right graph). *p < 0.0004, **p < 0.005

(C) IL-2 is polarized inward toward T-T contacts after PMA and ionomycin stimulation. DO11.10 CD4+ T cells were stimulated as in (A) and stained as in (B). IL-2 is shown on a grayscale in a z reconstruction of a large (left) and a small (right) cluster. IL-2 localization is graphically represented as the percent of IL-2+T cells pointing in toward a facing T cell (black bar) or pointing away from a neighboring T cell (gray bar). The average exposed surface was at least 50% for all of these measurements. p < 0.0001



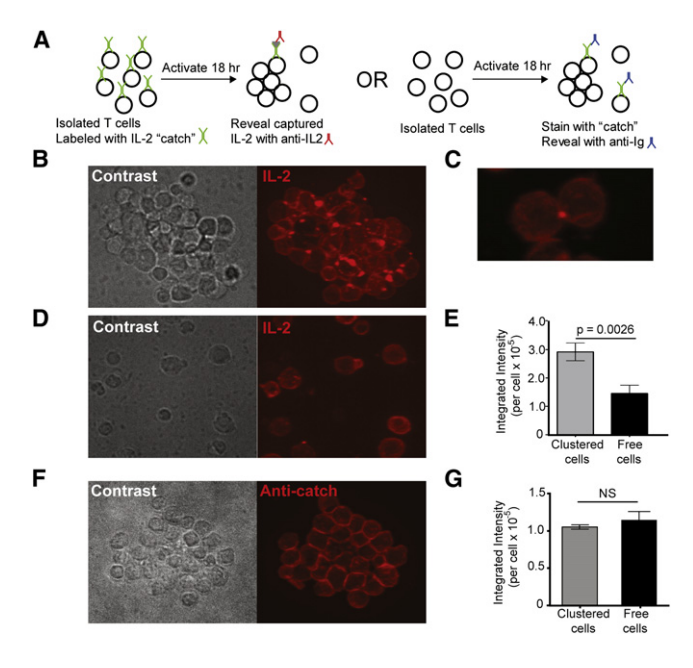


Figure 6. Preferential Capture of IL-2 within Synaptic Regions of T-T Clusters

(A) Scheme for identifying spatial parameters for IL-2 capture by T cells. (B–E) IL-2 "catch" reagent-coated BALB/c WT CD4+ T cells were stimulated with PMA and ionomycin for 19 hr, fixed with PFA, and stained with phycoerythrin-conjugated IL-2 detection antibody. Representative images of clustered cells (B and C) and free cells (D) and mean fluorescence intensity of IL-2 detection antibody staining per cell (n = 586 for clustered cells; n = 52 for free cells) (E) are shown. Data are representative of three independent experiments. (F and G) BALB/c CD4+ T cells were stimulated with PMA and ionomycin for 19 hr, fixed with PFA, coated with IL-2 catch reagent, and stained with rhodamine-conjugated secondary antibody against catch reagent (anti-catch). Representative image of clustered cells (F) and mean fluorescence intensity of secondary antibody staining per cell (n = 215 for clustered cells; n = 28 for free cells) (G) are shown.

All fluorescence images are maximum projection of z stacks. Error bars in (E) and (G) represent SD.

left), we were able to reveal accumulated IL-2 in clusters to determine whether T cells in these arrays were preferentially exposed to IL-2 relative to those that did not participate. This assay revealed that T cells in clusters (Figure 6B) accumulated puncta of IL-2 on their surface and that this surface accumulation was almost universally directed inward toward the cluster (isolated two-cell cluster shown in Figure 6C; see Movie S6 for 3D rendering). In contrast, cells from the same culture condition that were not involved in a cluster (Figure 6D) had 2-fold less fluorescence intensity per cell on average, a measure of the total amount of IL-2 captured (Figure 6E). The staining pattern for these was typically much more even, although faint puncta on the surface could occasionally be discerned, perhaps a result of a synaptic delivery during a transient encounter. To rule out the possibility of aggregation of the catch ligand itself in the synaptic space, we also coated cells with catch reagent after stimulation and fixing and stained with rhodamine-conjugated secondary antibody against catch reagent (Figure 6A, right). The bright puncta were not evident in clusters (Figure 6F), and the intensity of clustered and free cells for this marker was indistinguishable (Figure 6G). This supports the interpretation that IL-2 was locally captured on the catch reagents in Figure 6B and subsequently detected as T-T localized puncta. Furthermore, the data support that cells that are not engaged in synaptic contacts accumulate less synaptic IL-2 (indeed, also less overall; Figure 6E) as compared to synapse-engaged T cells.

IL-2 Signaling Is Polarized at T-T Synapses

The data above suggested a synaptic basis for IL-2 signaling between activated T cells. IL-2 binds to a nonsignaling alpha chain (CD25) as well as two signaling-competent beta and gamma chains (CD122 and CD132 [γc], respectively). Although antibodies against CD122 were not sensitive enough for staining, we found that both CD25 and CD132 were accumulated in the T-T interfaces, although the former in particular was not always uniformly expressed at high amounts, as it is upregulated to a varying extent in individual T cells over activation. Assessment of accumulation of surface proteins is difficult for multicellular clusters when all of the cells in the clusters express the receptor and is also subject to artifacts due to a local increase of total membrane in the synaptic region (typically, more than two cells contribute membrane to the same detection space). To control for this factor, we costained cells with lipophilic DilC, a far-red dye that intercalates into membranes and thus is a surrogate marker for local membrane density. We demonstrated that regions of T-T synapses were also enriched in DilC staining (Figure 7A). By comparing the normalized cell surface staining intensities along the surface to DilC staining, we demonstrated that CD25 enrichment typically was no greater in the synaptic region (highlighted by arrows) as compared to total membrane accumulation (Figure 7B) and may in fact be more highly represented outside of the contact region. In contrast, CD132, the signaling subunit, showed strong accumulation in the synaptic region, even when compared to the total membrane. This accumulation typically corresponded to a prominent dot, which was evident in the contacts as visualized with CD132 or in the CD132-DilC overlav.

IL-2 signaling through CD122 and the common gamma chain (CD132; γ c) triggers association of STAT5 with the membrane and coordinates its subsequent phosphorylation by Jak kinase family members (Lin and Leonard, 2000). When aggregated T-T clusters were stained for the phosphorylated form of STAT5 (p-STAT5), substantially more p-STAT5 accumulated within clustered T cells than in "free" cells found outside the confines of a cluster (Figures 7C and 7D). In contrast to free T cells, the mean fluorescence intensity (MFI) of p-STAT5 within clusters did not adhere to a normal distribution; rather, 37% of clustered cells were markedly brighter for p-STAT5 than the brightest free cell (Figure 7D).

In addition, the vast majority of clustered T cells examined showed p-STAT5 puncta facing inward toward other T cells, strongly suggesting a local activation of this molecule at the site of T-T contacts (Figures 7E and 7F). Some of these puncta also faced T-DC contacts, consistent with localized stimulation of γc cytokine receptors at these synapses. Similar to that seen with pericentrin (Figure 5A), p-STAT5 polarization was specific, irrespective of the available amount of T-T versus free membrane surface (Figure 7F). p-STAT5 and IL-2 were polarized in the same direction at T-T interfaces in 75% of interfaces analyzed (in 31 counted clusters) (Figure 7G). This polarization of



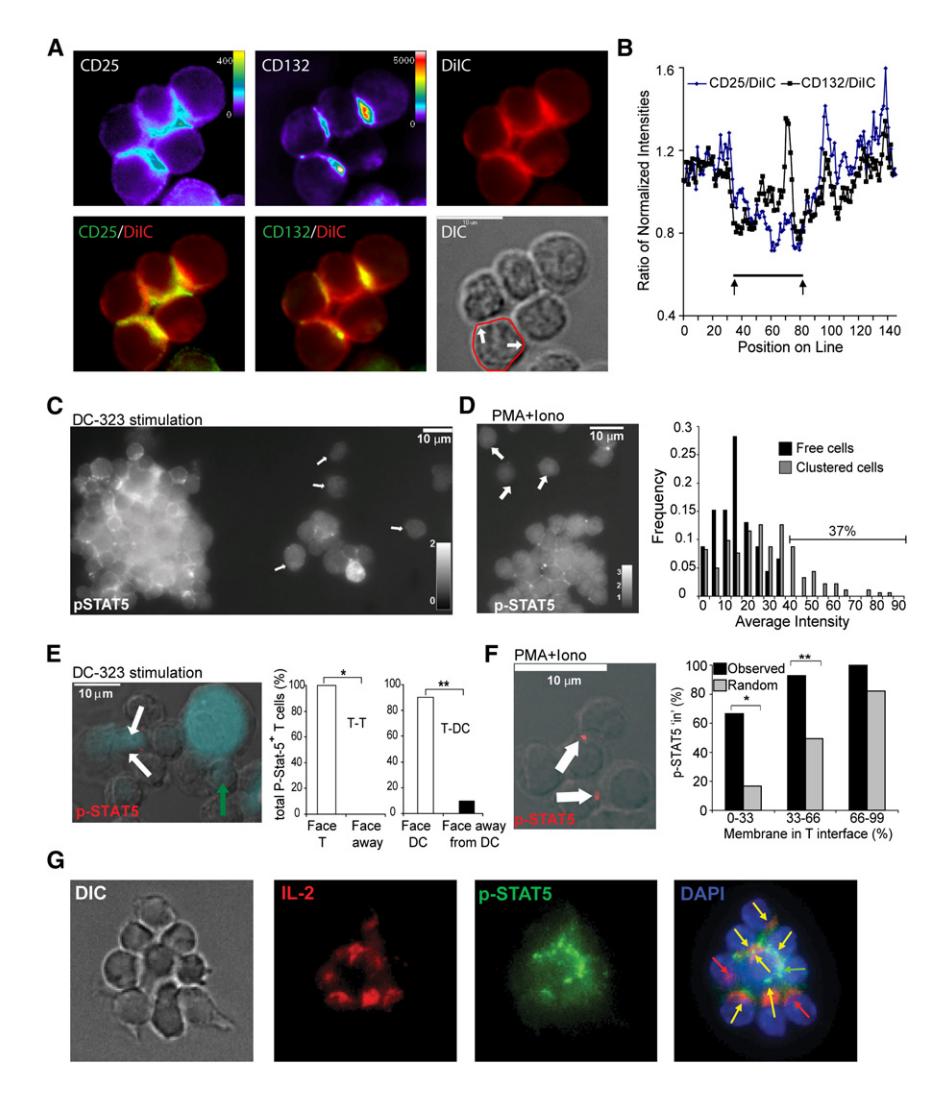


Figure 7. IL-2 Receptor Signaling across T-T Synapses

(A) Purified CD4⁺ T cells were activated for 19 hr with PMA and ionomycin and stained with antibodies to CD25 and CD132 and with the membrane-staining dye DilC. Overlays of CD25-DilC and CD132-DilC are shown in order to accentuate regions at which antibody staining intensity exceeded membrane intensity.

(B) A line scan (starting from at the back of the contact, shown overlaid onto the DIC image in [A]) of the membrane domain of a single T cell is shown compared for the three stains at the same focal place. Normalized intensities were compared on a pixel-by-pixel basis and demonstrate a peak of CD132 accumulation in the central contact region. (C and E) OT-II CD4+ T cells were activated for 20 hr with actin-CFP+ BMDCs prepulsed with OVA 323 (10 μg/ml). Permeabilized clusters were stained with anti-phospho-STAT5 antibody. In (C), the image is shown as a 3D maximal-intensity projection, and p-STAT5 stain is represented in white, with arrows indicating free cells. In (E), DCs are represented in blue on the wide-field DIC overlay with p-STAT5 antibody in red; white arrows indicate p-STAT5 localized in toward a DC, and the green arrow indicates p-STAT5 pointing inward toward a T cell. p-STAT5 localization is graphically represented as the percent of p-STAT5+ T cells pointing in toward a facing T cell (green bar) or pointing away from a neighboring T cell for all p-STAT5⁺ T-T pairs (left graph in [E]) and as the percent of p-STAT5+T cells pointing toward a DC (white bar) or away from the DC (black bar) for all p-STAT5+ T-DC pairs (right graph in [E]). *p < 0.008, **p < 0.00001.

(D and F) CD4⁺ T cells were activated for 19 hr with PMA and ionomycin. Clusters were harvested and stained as above. In (D), a 3D projection of the entire cell volume is shown, and p-STAT5 stain is represented in white, with arrows indicating free cells. The graph represents the frequency of p-STAT5 fluorescence intensities (with background

subtracted) for clustered (gray bars) and free (black bars) cells. In (F), p-STAT5 is red on the wide-field DIC overlay; white arrows indicate p-STAT5 localized in toward a T cell. The graph represents the actual percent of p-STAT5 facing "in" (black bars) versus the predicted percent of p-STAT5 that would be expected to face "in" (gray bars) if the polarization were due to the percent of available T-T membrane interface (x axis). *p = 0.0192, **p = 0.0011 by chi-square goodness-of-fit test.

(G) CD4⁺ T cells were stimulated with PMA and ionomycin for 18 hr and stained for anti-p-STAT5 and anti-IL-2; cells were costained with DAPI. Shown are DIC (leftmost panel); IL-2 (red, second panel from left); p-STAT5 (green, second panel from right); and an overlay of IL-2 (red), p-STAT5 (green), and DAPI (blue) (rightmost panel). Arrows indicate the following: green, localization of p-STAT5 only; red, localization of IL-2 only; yellow, colocalization of p-STAT5 and IL-2. Scale bars = 10 μm. Data are representative of two independent experiments.

p-STAT5 and IL-2 toward one another on facing T cells is similar to the mutual exclusion of IL-2 production and STAT5 activation observed by flow cytometry in previous studies (Long and Adler, 2006) and emphasizes the importance of paracrine IL-2 signaling in facilitating T cell activation. Thus, T-T synapses facilitate synapse-based IL-2 signaling, consistent with polarized secretion from the cells across the synapse.

DISCUSSION

T-T clusters have long been considered a correlate of efficient T cell activation. Here, we supply new evidence that activated T cell clusters result in the establishment of multifocal synapses through which cytokines are directionally shared. These con-

tacts are synapses by a number of distinct criteria used to compare neuronal and immunological synapses (Dustin and Colman, 2002). These include that they are dynamic but stabilized, utilize adhesive LFA-1 molecules for their formation, retain their distinct identities with a gap between their apposed membrane surfaces, and most importantly meet the functional criteria of facilitating directed secretion via polarizing the MTOC as well as signaling molecules IL-2 and p-STAT5. We also provide evidence that these interactions are functionally important insofar as T cells that form these contacts generate stronger signals compared to those that activate without cell-cell contact.

Interestingly, T-T association in vivo and in vitro occurs not only during stable interactions with APCs but also during swarming interactions, when clusters are dynamic. Recent evidence



suggests that the IS between a T cell and APC is in fact a more dynamic structure than initially recognized, with PKC0-driven migration phases required for IL-2 production (Sims et al., 2007). Transient interactions between T cells and APCs have been described as a period for augmentation of antigenic signals (Miller et al., 2004) and may, in the case of T-T interactions, be used for enhanced IL-2 signaling and subsequent T cell activation, potentially at the onset of proliferation.

The specificity by which activated T cells cluster remains to be discovered. Our data show, as has been demonstrated previously (Rothlein and Springer, 1986; Rothlein et al., 1986; van Kooyk et al., 1989), that LFA-1 interactions between T cells are an integral part of assembly. Although the upregulation of both LFA-1 avidity and ICAM-1 expression during activation may in part mediate specificity such that already activated T cells tend to synapse (Rothlein et al., 1986), it is also possible that a unique class of activation-driven receptors that favor synaptic interactions remain to be identified. In this light, γc cytokines are not themselves required for T-T interactions (C.A.S., J.D., and M.F.K., unpublished data).

The localized distribution of γc cytokine receptors in T cells activated in the context of a cell-cell contact also represents an expansion of the complexity of this signaling pathway. Although our data demonstrate clearly enhanced amounts of p-STAT5 in T cell clusters overall and a substantial amount of this within the nuclear region, we were surprised by the enrichment of the phosphorylated (active) form directly adjacent to the receptor. This observation in particular may indicate that the localization of activating cytokine receptors along the membrane may generate signalosomes whose molecular players are determined by a wider variety of signaling receptors than the cytokine itself. Unique localization in a synapse may thus underlie the unique outcomes of IL-2 and IL-15 signaling, both of which are generated in part through STAT5 (Lin and Leonard, 2000).

The T-T synaptic localization of cytokines and their receptors may also support the "transpresentation" of γc cytokines on their alpha chains. Recently, it has been shown that the IL-2Ra chain in particular is critical in driving T cell help for the establishment of CD8+ T cell effector functions and memory (Janssen et al., 2005; Williams et al., 2006) and that this can be mimicked by anti-IL-2-IL-2 antibody complexes (Boyman et al., 2006) when the Fc portion of IL-2 antibody is preserved. The IL-2 crystal structure revealed that binding of IL-2Rα to IL-2 may stabilize a secondary binding site for presentation to IL-2R β , with γ c subsequently recruited by this complex (Wang et al., 2005). Similarities in the carboxyl termini of IL-15Rα (known to transpresent IL-15) and IL-2R α have strengthened the notion that IL-2 may also be presented in trans (Chirifu et al., 2007). In our data, it is notable that the accumulation of the gamma chain (CD132) was much more pronounced than for the alpha chain (CD25), perhaps suggesting that only the former is clustered whereas the latter "catches" IL-2, perhaps relatively independently. Alternatively, the localized secretion of IL-2 seen at these tight T-T junctions may negate the need for IL-2Rα transpresentation and allow for direct IL-2 β/γ c signaling.

Paracrine IL-2 has been shown to be sufficient for a fully functional CD8 $^+$ memory T cell response in the case of a primary helpless stimulation (Williams et al., 2006), a function that could be fulfilled by CD4 $^+$ T cells directing or presenting IL-2 to CD8 $^+$ T

cells using the mechanism elaborated here. Chemokine-mediated attraction of naive CD8⁺ T cells to areas of activated CD4⁺ T-DC interactions has been described recently (Castellino et al., 2006), and T-T interactions may facilitate the sharing of IL-2 in this context.

The data presented herein are consistent with previous reports showing that IL-2 polarizes toward APCs (Huse et al., 2006) but also present the important extension that IL-2 secretion is also specifically polarized between adjacent T cells. They are also highly consistent with flow cytometry experiments demonstrating that IL-2-producing cells are rarely enriched with p-STAT5 (Long and Adler, 2006), a result that may, in this light, be caused by synaptic interactions between IL-2 producers and those that do not produce the cytokine but rather receive the resultant signals. In the case of a number of cytokines for which receptors lie only on other T cells and not on APCs, this may represent an important means of influencing the activation and differentiation of neighboring cells. In particular, T helper cell cytokine feedback may allow a collection of clones to come to a quorum decision and/or assist a preexisting differentiated clone to influence the response of newly activating clones.

Our results here remain to be extended to known pathogenic and clonally diverse situations. It is clear that our studies utilize high precursor frequencies for a single peptide and would typically be higher than a normal naive repertoire for pathogens. The inflammatory chemokines CCL3 and CCL4 have been shown to attract activating T cells toward one another (Castellino et al., 2006; Hugues et al., 2007) and may play a role in enhancing synaptic exchange of cytokines. Notably, though, the mechanism we describe may have greatest relevance in secondary responses or when expanded memory effector cells are activated alongside new clones. We have also recently detected clusters with similar dynamics in polyclonal T cell populations in the draining LN during secondary responses to lymphocytic choriomeningitis virus (R.S.F., J. Hu, M.F.K., and M. Mattloubian, unpublished data). Synaptic contacts may, in this context, assist lower-affinity clones or boost stimulation as antigen concentrations decrease postinfection. As such, the cell biology of T-T synapses is likely to prove important in numerous other immunological settings.

EXPERIMENTAL PROCEDURES

Mice

BALB/c, C57BL/6, Actin-CFP, LFA-1-deficient $Itgb2^{-/-}$, DO11.10 TCR transgenic, and OT-II TCR transgenic mice were purchased from The Jackson Laboratory. DO11.10 mice, which express a TCR specific for chicken ovalbumin amino acids 323–339 (referred to as "OVA 323" here) in the context of MHC class II molecule I-A^d, were crossed with BALB/c mice to obtain heterozygous DO11.10 mice. OT-II transgenic mice also express an OVA peptide-specific TCR that pairs with the CD4 coreceptor in the context of MHC class II molecule I-A^b; OT-II mice were crossed with C57BL/6 mice to obtain heterozygous OT-II mice. Actin-CFP mice express a transgenic construct containing an enhanced cyan fluorescent protein gene under the control of a chicken β -actin promoter coupled with the cytomegalovirus (CMV) immediate early enhancer. CD11c-YFP mice (Lindquist et al., 2004) were a kind gift of M. Nussenzweig. All mice were bred and maintained in accordance with the guidelines of the Lab Animal Resource Center of the University of California, San Francisco.

Antibodies

Anti-LFA-1 (M17/4), fluorescein isothiocyanate-conjugated monoclonal anti-CD25 (2A3), and biotinylated anti-IL-2 (JES6-5H4) were obtained from BD



PharMingen. Biotinylated polyclonal anti-IL-15R α was obtained from R&D Systems. Anti-phospho-STAT5 (Tyr694) was obtained from Cell Signaling Technology. Polyclonal anti-pericentrin was obtained from Covance. Secondary antibodies (Jackson Immunoresearch) utilized were rhodamine-conjugated donkey anti-rat, rhodamine-conjugated donkey anti-goat, and rhodamine-conjugated streptavidin. Anti-CD3 (500.A2) and anti-CD28 (37N51.1) antibodies were prepared from cultured hybridoma supernatant using standard protein A/G antibody purification methods.

Immunocytochemistry

CD4+ T cells were purified from spleen and lymph node (LN) cells from DO11.10 and OT-II mice by negative selection using a CD4⁺ negative selection StemSep purification kit (Stem Cell Technologies, Inc.) or a MACS kit (Miltenyi Biotec) with MACS LS+ selection columns. Purified CD4 $^+$ T cells (4 \times 10 5) were activated in 96-well flat-bottom plates (Fisher Scientific) for 19-20 hr at 37°C, 5% CO₂ with 10 ng/ml PMA (Sigma-Aldrich) and 0.5 μg/ml ionomycin (Sigma-Aldrich) or actin-CFP⁺ BMDCs (1 × 10⁵) (grown in GM-CSF and IL-4; LPS-matured) and were prepulsed with OVA peptide (10 µg/ml; AnaSpec). Medium used was RPMI 1640 (GIBCO) supplemented with 10% fetal calf serum (JRH Biosciences), L-glutamine (2 mM; UCSF Cell Culture Facility), penicillin/streptomycin (100 units/ml and 100 $\mu g/ml$, respectively; GIBCO), and β mercaptoethanol (50 μM; Sigma) (R10 medium). Staining was then performed at room temperature (RT). Briefly, cell clusters were gently harvested and fixed to polylysine-coated Superfrost slides (VWR) with 1% paraformaldehyde (PFA; Electron Microscopy Services) for 10 min, and slides were then centrifuged to adhere the cells to the slide. Fixed cells were blocked in wash buffer with 1% FCS (and 2% normal donkey serum for slides where secondary donkey antibodies were used) and permeabilized for 30 min with 0.02% saponin (Sigma) in PBS. Cells were incubated for 60 min with primary antibodies, washed extensively, and stained with secondary antibody for 60 min. DAPI (4',6-diamidino-2-phenylindole) was used in the final wash where indicated. Cells were then washed overnight and treated with antifade reagent (Bio-Rad), after which slides were sealed and imaged. A modified Zeiss Axiovert 200M microscope with a Plan Neofluar 40X objective was used for imaging experiments. The microscope was fitted with dual excitation and emission filter wheels and a Photometrics Coolsnap HQ camera. The imaging and control software used was MetaMorph (Universal Imaging, Molecular Devices Corp.).

For experiments where DilC was used to quantify membrane, cells were stained with DilC (DilC₁₈, 1,1'-dioctadecyl-3,3,3',3'-tetramethylindocarbocyanine perchlorate, Invitrogen) for 5 min at RT prior to fixation and staining.

To determine the percentage of total pericentrin-, IL-2-, or p-STAT5-positive T cells with pericentrin, IL-2, or p-STAT5 facing toward or away from another T cell, only the cells in the outermost layer of a cluster (i.e., where the marker could potentially face toward or away from an adjacent cell) were counted. The marker was scored as facing toward an adjacent T cell fi it was within the first third of the cell membrane juxtaposed to another T cell membrane. To determine the percentage of total IL-2- or p-STAT5-positive T cells with IL-2 or p-STAT5 facing toward or away from a DC, all cells were counted, as in all instances the marker could potentially face toward or away from the DC. Line scans were performed in MetaMorph, and intensities along the line were normalized by dividing by the sum of the total intensities of all points along the membrane.

Electron Microscopy

 12×10^6 BALB/c WT CD4 $^+$ T cells were stimulated with PMA (5 ng/ml) and ionomycin (125 ng/ml) in 3 ml of R10 medium in a six-well plate. Eighteen hours poststimulation, 3 ml of prewarmed 3% glutaraldehyde/1% PFA (0.1 M cacodylate buffer [pH 7.4]) was applied, and cells were fixed at 37° C for 20 min and stored at 4° C. Fixed cells were then rinsed in water, postfixed in reduced OsO4 (2% OsO4 + 1.5% potassium ferrocyanide, Sigma, prepared fresh), and stained en bloc with uranyl acetate before being dehydrated in ethanol, cleared in propylene oxide, and embedded in eponate 12 (Ted Pella Co.). Thin sections were cut with a Leica Ultracut UCT microtome and examined under a Philips Tecnai 10 electron microscope.

Cluster Analysis

Purified CD4⁺ DO11.10 TCR transgenic T cells were stimulated with PMA and ionomycin as described above or with plate-bound CD3 antibody (flat-bottom

96 well plates precoated with 50 μ l/well antibody for 1 hr at 37 $^{\circ}$ C or overnight at 4 $^{\circ}$ C and washed extensively) in titrated concentrations from 0.1 to 1 μ g/ml and soluble CD28 antibody (added at beginning of assay at 5 μ g/ml). LFA-1 antibody (20 μ g/ml) was added 18 hr after initial stimulation, and wells were photographed at 20 hr. Wells were photographed at 1–4 spots per well (2–3 wells per condition) at noted the time points, and cluster area was measured with MetaMorph software. Where indicated, BMDCs were labeled with CMAC (7-amino-4-chloromethylcoumarin, Invitrogen).

For time-lapse microscopy of clusters, CD4 $^{+}$ T cells were purified from C57BL/6 mice, and some of the purified T cells were labeled with carboxyfluor-escein diacetate succinimidyl ester (CFSE; Invitrogen). 3 \times 10 5 T cells (90% unlabeled and 10% CFSE labeled, in R10 medium with 0.1% low-melt agarose) were stimulated by PMA (5 ng/ml) and ionomycin (125 ng/ml) in eight-well Lab-Tek chambers (Nunc). Time-lapse microscopy was performed 18 hr after stimulation.

IL-2 Capture Assay

CD4+ T cells purified from BALB/c WT mice were coated with mouse IL-2 catch reagent from a mouse IL-2 secretion assay detection kit (Miltenyi Biotec) by incubating T cells in a 20× dilution of IL-2 catch reagent in R10 medium for 15 min in ice and washing once with R10 medium. Then, the IL-2 catch reagent-coated T cells were stimulated with PMA/ionomycin in a flat-bottom 96-well plate for 19 hr. Activated T cells were transferred to eight-well Lab-Tek chambered coverslips (Nunc) coated with polylysine, incubated 15 min at 37°C with 5% CO₂, spun at 1500 rpm for 5 min, fixed with 1% PFA for 15 min at 4°C, and stained with phycoerythrin-conjugated IL-2 detection antibody (1:20 dilution in R10 medium). Finally, 1% low-melt agarose was added to the wells, and Lab-Tek wells were spun at 1500 rpm at RT. Samples embedded in agarose gel were examined with a spinning disk confocal microscope (Yogogawa). Single-plane bright-field images and z stacks of red fluorescence images (0.4 μm intervals) were acquired with a 40× objective lens (Nikon, NA 1.3). Acquired images were analyzed using MetaMorph. Fluorescence intensity was integrated over the volume of single cells or clustered cells after background subtraction. For clustered cells, the integrated fluorescence intensity was divided by the number of cells in the clusters to obtain integrated fluorescence intensity per cell.

Statistical Analyses

The chi-square test and Student's t test were utilized as indicated in the text. All p values < 0.05 were considered significant.

TPLSM Acquisition

CD4⁺ T cells purified from DO11.10 or OT-II mice as described above were labeled with CFSE (carboxyfluorescein diacetate succinimidyl ester, Invitrogen) or CMTMR (5-(and-6)-[4-chloromethyl(benzoyl)amino] tetramethylrhodamine, Invitrogen) at 5 μ M for 10 min at RT. Cells were washed extensively, and 5×10^6 dye-labeled cells were intravenously transferred to WT BALB/c or C57BL/6 CD11c-YFP recipients. Twenty-four hours later, mice were immunized s.c. in the footpads with 25 µg OVA peptide emulsified in CFA (Sigma) or PBS-CFA as a control or were left unimmunized as a control. A further 24 hr later, popliteal LNs were immobilized on coverslips with the hilum facing away from the objective. A custom resonant-scanning instrument (Tang et al., 2006) containing a four-photomultiplier tube operating at video rate was used for two-photon microscopy. LNs were maintained at 36°C in RPMI medium bubbled with 95% O₂/5% CO₂ and were imaged through the capsule distal to the hilum. Samples were excited with a 5 W Mai Tai Ti:Sapphire laser (Spectra-Physics) tuned to a wavelength of 810 nm, and emission wavelengths of 500-540 nm (for CFSE) and 380-420 nm (for detection of second-harmonic emission) were collected. A custom four-dimensional acquisition module in VideoSavant digital video recording software (IO Industries) was utilized for image acquisition. Each LN was first surveyed in a raster scan for the presence of transferred cells. Adjacent z stacks of up to 350 µm encompassing the top xy space of the LN were collected. For time-lapse acquisition, each xy plane spanned 330 μ m \times 230 μ m at a resolution of 0.6 μ m per pixel, and ten video-rate frames were averaged, giving an effective collection time of approximately 330 ms per image. Images of up to 30 xy planes with 5 μm z spacing were acquired every 30 s for 30 min. Images were analyzed with Imaris



Dwell time of T-T interactions was measured by tracking the length of time that a given T cell remained in close association (<10 $\mu m)$ with another T cell. The measured value does not consider additional numbers of associated cells. For example, in some images, a T cell pair joined a second T-T pair and then separated. When each pair still retained a T-T contact, this additional contact was not considered, and the dwell time represents when a given T cell ceased to have any T-T association.

SUPPLEMENTAL DATA

Supplemental Data include one figure and six movies and can be found with this article online at http://www.immunity.com/cgi/content/full/29/2/238/DC1/.

ACKNOWLEDGMENTS

C.A.S. performed TPLSM imaging, immunocytochemistry experiments for LFA-1, CD25, pericentrin, p-STAT5, and IL-2, and data analysis and participated in experimental design and manuscript writing. J.D. performed TPLSM imaging, electron microscopy, immunocytochemistry experiments for p-STAT5, intracellular and capture IL-2 stains, LFA-deficient cluster experiments and analysis, and participated in experimental design and manuscript writing. S.C. performed clustering experiments and immunocytochemistry for LFA-1 and CD25 and participated in experimental design and data analysis. R.S.F. performed TPLSM for nonimmunized mice and assisted in manuscript writing lished the initial TPLSM work and provided technical assistance. M.F.K. established the initial scientific questions, provided continuing intellectual guidance, and participated in experimental design, analysis, manuscript writing, and TPLSM imaging.

We would like to thank F. Siedenberg and L. Braun (Sutter Instruments) for technical assistance, I. Hsieh for assistance with electron microscopy, A. Hedges (University of Bristol) for assistance with statistics, and A. Ma and A. Abbas for helpful discussions. This work was supported by NIH training grant #5T32Al007334 (C.A.S.), a National Multiple Sclerosis Society Postdoctoral Fellowship (S.C.), startup funds from the HHMI Biomedical Research Support Program (grant #5300246), and the Juvenile Diabetes Foundation (M.F.K.).

Received: March 31, 2007 Revised: March 27, 2008 Accepted: May 12, 2008 Published online: July 31, 2008

REFERENCES

Bousso, P., and Robey, E. (2003). Dynamics of CD8(+) T cell priming by dendritic cells in intact lymph nodes. Nat. Immunol. 4, 579–585.

Boyman, O., Kovar, M., Rubinstein, M.P., Surh, C.D., and Sprent, J. (2006). Selective stimulation of T cell subsets with antibody-cytokine immune complexes. Science *311*, 1924–1927.

Brossard, C., Feuillet, V., Schmitt, A., Randriamampita, C., Romao, M., Raposo, G., and Trautmann, A. (2005). Multifocal structure of the T cell - dendritic cell synapse. Eur. J. Immunol. *35*, 1741–1753.

Bunnell, S.C., Hong, D.I., Kardon, J.R., Yamazaki, T., McGlade, C.J., Barr, V.A., and Samelson, L.E. (2002). T cell receptor ligation induces the formation of dynamically regulated signaling assemblies. J. Cell Biol. *158*, 1263–1275.

Castellino, F., Huang, A.Y., Altan-Bonnet, G., Stoll, S., Scheinecker, C., and Germain, R.N. (2006). Chemokines enhance immunity by guiding naive CD8+ T cells to sites of CD4+ T cell-dendritic cell interaction. Nature *440*, 890–895

Chirifu, M., Hayashi, C., Nakamura, T., Toma, S., Shuto, T., Kai, H., Yamagata, Y., Davis, S.J., and Ikemizu, S. (2007). Crystal structure of the IL-15-IL-15Ralpha complex, a cytokine-receptor unit presented in trans. Nat. Immunol. *8*, 1001–1007.

Dustin, M.L., and Colman, D.R. (2002). Neural and immunological synaptic relations. Science 298, 785–789.

Grakoui, A., Bromley, S.K., Sumen, C., Davis, M.M., Shaw, A.S., Allen, P.M., and Dustin, M.L. (1999). The immunological synapse: a molecular machine that controls T cell activation. Science *285*, 221–226.

Hommel, M., and Kyewski, B. (2003). Dynamic changes during the immune response in T cell-antigen-presenting cell clusters isolated from lymph nodes. J. Exp. Med. 197, 269–280.

Hugues, S., Fetler, L., Bonifaz, L., Helft, J., Amblard, F., and Amigorena, S. (2004). Distinct T cell dynamics in lymph nodes during the induction of tolerance and immunity. Nat. Immunol. *5*, 1235–1242.

Hugues, S., Scholer, A., Boissonnas, A., Nussbaum, A., Combadiere, C., Amigorena, S., and Fetler, L. (2007). Dynamic imaging of chemokine-dependent CD8+ T cell help for CD8+ T cell responses. Nat. Immunol. 8, 921–930.

Huppa, J.B., Gleimer, M., Sumen, C., and Davis, M.M. (2003). Continuous T cell receptor signaling required for synapse maintenance and full effector potential. Nat. Immunol. *4*, 749–755.

Huse, M., Lillemeier, B.F., Kuhns, M.S., Chen, D.S., and Davis, M.M. (2006). T cells use two directionally distinct pathways for cytokine secretion. Nat. Immunol. 7, 247–255.

Inaba, K., Witmer, M.D., and Steinman, R.M. (1984). Clustering of dendritic cells, helper T lymphocytes, and histocompatible B cells during primary antibody responses in vitro. J. Exp. Med. *160*, 858–876.

Ingulli, E., Mondino, A., Khoruts, A., and Jenkins, M.K. (1997). In vivo detection of dendritic cell antigen presentation to CD4(+) T cells. J. Exp. Med. *185*, 2133–2141.

Janssen, E.M., Droin, N.M., Lemmens, E.E., Pinkoski, M.J., Bensinger, S.J., Ehst, B.D., Griffith, T.S., Green, D.R., and Schoenberger, S.P. (2005). CD4+ T-cell help controls CD8+ T-cell memory via TRAIL-mediated activation-induced cell death. Nature *434*. 88–93.

Krummel, M.F., Sjaastad, M.D., Wülfing, C., and Davis, M.M. (2000). Differential clustering of CD4 and CD3zeta during T cell recognition. Science 289, 1349–1352.

Kupfer, A., Dennert, G., and Singer, S.J. (1983). Polarization of the Golgi apparatus and the microtubule-organizing center within cloned natural killer cells bound to their targets. Proc. Natl. Acad. Sci. USA *80*, 7224–7228.

Lin, J.X., and Leonard, W.J. (2000). The role of Stat5a and Stat5b in signaling by IL-2 family cytokines. Oncogene 19, 2566–2576.

Lindquist, R.L., Shakhar, G., Dudziak, D., Wardemann, H., Eisenreich, T., Dustin, M.L., and Nussenzweig, M.C. (2004). Visualizing dendritic cell networks in vivo. Nat. Immunol. 5, 1243–1250.

Long, M., and Adler, A.J. (2006). Cutting edge: Paracrine, but not autocrine, IL-2 signaling is sustained during early antiviral CD4 T cell response. J. Immunol. 177, 4257–4261.

Mempel, T.R., Henrickson, S.E., and von Andrian, U.H. (2004). T-cell priming by dendritic cells in lymph nodes occurs in three distinct phases. Nature 427, 154–159.

Miller, M.J., Wei, S.H., Parker, I., and Cahalan, M.D. (2002). Two-photon imaging of lymphocyte motility and antigen response in intact lymph node. Science 296, 1869–1873.

Miller, M.J., Wei, S.H., Cahalan, M.D., and Parker, I. (2003). Autonomous T cell trafficking examined in vivo with intravital two-photon microscopy. Proc. Natl. Acad. Sci. USA 100, 2604–2609.

Miller, M.J., Safrina, O., Parker, I., and Cahalan, M.D. (2004). Imaging the single cell dynamics of CD4+ T cell activation by dendritic cells in lymph nodes. J. Exp. Med. 200, 847–856.

Monks, C.R., Freiberg, B.A., Kupfer, H., Sciaky, N., and Kupfer, A. (1998). Three-dimensional segregation of supramolecular activation clusters in T cells. Nature *395*, 82–86.

Pentcheva-Hoang, T., Egen, J.G., Wojnoonski, K., and Allison, J.P. (2004). B7-1 and B7-2 selectively recruit CTLA-4 and CD28 to the immunological synapse. Immunity *21*, 401–413.



Rothlein, R., and Springer, T.A. (1986). The requirement for lymphocyte function-associated antigen 1 in homotypic leukocyte adhesion stimulated by phorbol ester. J. Exp. Med. 163, 1132-1149.

Rothlein, R., Dustin, M.L., Marlin, S.D., and Springer, T.A. (1986). A human intercellular adhesion molecule (ICAM-1) distinct from LFA-1. J. Immunol. 137, 1270-1274.

Shakhar, G., Lindquist, R.L., Skokos, D., Dudziak, D., Huang, J.H., Nussenzweig, M.C., and Dustin, M.L. (2005). Stable T cell-dendritic cell interactions precede the development of both tolerance and immunity in vivo. Nat. Immunol. 6, 707-714.

Sims, T.N., Soos, T.J., Xenias, H.S., Dubin-Thaler, B., Hofman, J.M., Waite, J.C., Cameron, T.O., Thomas, V.K., Varma, R., Wiggins, C.H., et al. (2007). Opposing Effects of PKCtheta and WASp on symmetry breaking and relocation of the immunological synapse. Cell 129, 773-785.

Stinchcombe, J.C., Majorovits, E., Bossi, G., Fuller, S., and Griffiths, G.M. (2006). Centrosome polarization delivers secretory granules to the immunological synapse. Nature 443, 462-465.

Tang, Q., Adams, J.Y., Tooley, A.J., Bi, M., Fife, B.T., Serra, P., Santamaria, P., Locksley, R.M., Krummel, M.F., and Bluestone, J.A. (2006). Visualizing regulatory T cell control of autoimmune responses in nonobese diabetic mice. Nat. Immunol. 7, 83–92.

van Kooyk, Y., van de Wiel-van Kemenade, P., Weder, P., Kuijpers, T.W., and Figdor, C.G. (1989). Enhancement of LFA-1-mediated cell adhesion by triggering through CD2 or CD3 on T lymphocytes. Nature 342, 811-813.

Wang, X., Rickert, M., and Garcia, K.C. (2005). Structure of the quaternary complex of interleukin-2 with its alpha, beta, and gammac receptors. Science 310, 1159-1163.

Williams, M.A., Tyznik, A.J., and Bevan, M.J. (2006). Interleukin-2 signals during priming are required for secondary expansion of CD8(+) memory T cells. Nature 441, 890-893.